A Journal of the Gesellschaft Deutscher Chemiker

Angewandte Chemie

GDCh

International Edition

www.angewandte.org

## Accepted Article

**Title:** Bipyridine-assisted assembly of Au nanoparticles on Cu nanowires to enhance electrochemical reduction of CO2

**Authors:** Jiaju Fu, Wenlei Zhu, Ying Chen, Zhouyang Yin, Yuyang Li, Juan Liu, Hongyi Zhang, Junjie Zhu, and Shouheng Sun



**To be cited as:** *Angew. Chem. Int. Ed.* 10.1002/anie.201905318
*Angew. Chem.* 10.1002/ange.201905318

**Link to VoR:** http://dx.doi.org/10.1002/anie.201905318
http://dx.doi.org/10.1002/ange.201905318

WILEY-VCH

10.1002/anie.201905318

WILEY-VCH

COMMUNICATION

# Bipyridine-assisted assembly of Au nanoparticles on Cu nanowires to enhance electrochemical reduction of $CO_2$

Jiaju Fu[a, b, ‡], Wenlei Zhu[a, ‡], Ying Chen[b], Zhouyang Yin[a], Yuyang Li[a], Juan Liu[b], Hongyi Zhang[a], Jun-Jie Zhu*[b] and Shouheng Sun*[a]

**Abstract:** We report a new strategy to prepare a composite catalyst for highly efficient electrochemical $CO_2$ reduction reaction ($CO_2RR$). The composite catalyst is made by anchoring Au nanoparticles on Cu nanowires via 4,4'-bipyridine (bipy). The Au-bipy-Cu catalyzes the $CO_2RR$ to C-products in 0.1 M $KHCO_3$ with a total Faradaic efficiency (FE) reaching 90.6% at −0.9 V among which $CH_3CHO$ (25% FE) dominates the liquid product ($HCOO^-$, $CH_3CHO$, and $CH_3COO^-$) distribution (75%). The enhanced $CO_2RR$ catalysis demonstrated by Au-bipy-Cu originates from its synergistic Au ($CO_2$ to CO) and Cu (CO to C-products) catalysis which is further promoted by bipy. The Au-bipy-Cu represents a new catalyst system for effective $CO_2RR$ conversion to C-products.

Electrochemical $CO_2$ reduction reaction ($CO_2RR$) under ambient conditions is an important approach to understand $CO_2RR$ and to improve $CO_2RR$ conversion efficiency for renewable energy applications.[1] Past studies on electrochemical $CO_2RR$ have shown that it is possible to convert $CO_2$ to CO with high activity and selectivity on metal-based nanostructured surfaces.[2] However to convert $CO_2$ efficiently to hydrocarbon products has been challenging. Nanostructured Cu must be present and the side reaction, hydrogen evolution reaction (HER), in the aqueous electrolyte solution often competes with the main $CO_2RR$, lowering the $CO_2RR$ selectivity and efficiency,[3] unless CO is reduced directly[4]. Here we report the enhanced $CO_2RR$ catalysis of the Au-Cu composite catalyst for the selective formation of C-products. In this study, we assembled Au NPs on Cu NWs using 4,4'-bipyridine (bipy) as a linker, forming a new composite catalyst Au-bipy-Cu (**Figure 1a**). The electrochemical $CO_2RR$ in aqueous solution of 0.1 M $KHCO_3$ showed Au/Cu mass-dependent selectivity with Au/Cu =1/2 ratio yielding the highest selectivity to C-products with a total FE of 90.6% at −0.9 V (vs. RHE, same hereinafter) among which $CH_3CHO$ (25% FE) dominates the liquid product ($HCOO^-$, $CH_3CHO$, and $CH_3COO^-$) distribution (75%). Our studies demonstrate a new approach to tune synergistic catalysis of the Au-bipy-Cu composite catalyst for selective electrochemical $CO_2RR$ to hydrocarbons or oxygenated-hydrocarbons.

[a] J. Fu, Dr. W. Zhu, Z. Yin, Y. Li, Dr. H. Zhang and Prof. S. Sun
Department of Chemistry
Brown University
Providence, Rhode Island 02912, United States
E-mail: ssun@brown.edu
[b] J. Fu, Y. Chen, J. Liu and Prof. J. J. Zhu
State Key Laboratory of Analytical Chemistry for Life Science
School of Chemistry and Chemical Engineering,
Nanjing University
Nanjing 210023, China
E-mail: jjzhu@nju.edu.cn
[‡] These authors contribute equally to this work.

Supporting information for this article can be found under:

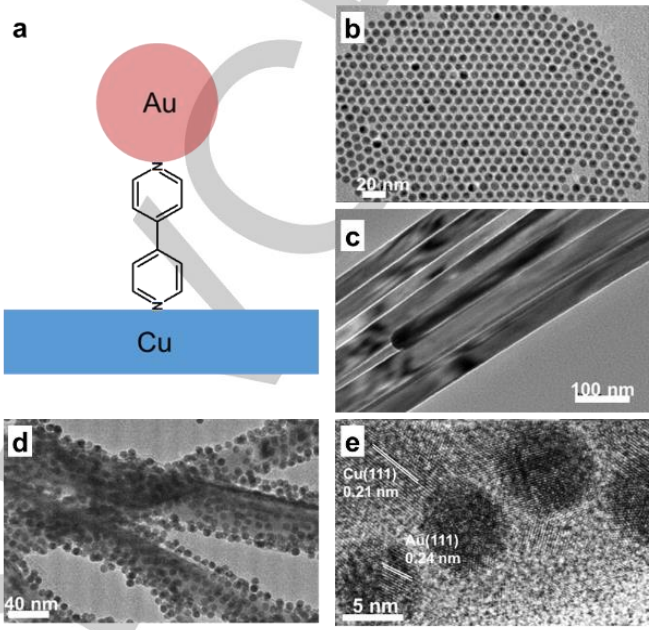


**Figure 1**. (a) Schematic illustration of Au-bipu-Cu composite catalyst. (b-d) TEM images of (b) 8 nm Au NPs, (c) 50 nm wide Cu NWs and (d) Au-bipy-Cu-1/1. (e) HRTEM image of a local area of Au-bipy-Cu-1/2.

8 nm Au NPs and 50 nm wide Cu NWs were specifically selected to make Au-bipy-Cu as the Au NPs have been demonstrated to be efficient for $CO_2$ reduction to CO[2a] and 50 nm wide Cu NWs were more selective for CO reduction to $C_2$-hydrocarbons.[5] Monodispersed 8 nm Au NPs were synthesized by reduction of $HAuCl_4$ with borane *tert*-butylamine complex in a solution mixture of oleylamine and 1,2,3,4-tetrahydronaphthalene as reported.[2a] 50 nm wide Cu NWs were synthesized by reduction of CuCl with oleylamine at 180°C, which was modified from the reported method.[6] Transmission electron microscopy (TEM) images of 8 nm Au NPs and 50 nm wide Cu NWs are shown in **Figure 1b&c** respectively. To prepare Au-bipy-Cu, Cu NWs or Au NPs was dispersed in a chloroform solution of 100 mM bipy and the mixture was stirred at room temperature for 12 h (to prepare Cu-bipy) or 6 h (to prepare Au-bipy). Then the Au-bipy and Cu-bipy were mixed together in chloroform at 25°C and stirred for 6 h to obtain Au-bipy-Cu. The mass ratio of Au/Cu in the Au-bipy-Cu was controlled by the amount of Au NPs and Cu NWs added in the assembly process, and was determined by inductively coupled plasma - atomic emission spectroscopy (ICP-AES). We found that in the Au/Cu mass ratios between 1/1 – 1/3, the Au NPs and Cu NWs were all included in the final Au-bipy-Cu composites. Therefore, we denote the composites as Au-bipy-Cu-1/1 (**Figure S1a**), Au-bipy-Cu-1/2 (**Figure 1d**), and Au-bipy-Cu-1/3 (**Figure S1b**) respectively. As a comparison, simply mixing Au NPs and Cu NWs without the bipy treatment gave only the random mixture of NPs and NWs (**Figure S2**). High-resolution TEM (HRTEM)

10.1002/anie.201905318


image of the Au-bipy-Cu-1/2 (**Figure 1e**) shows that after Au NP coupling to Cu NW via bipy, the lattice spacing of Au (111) and Cu (111) are measured to be 0.24 and 0.21 nm respectively, which are very close to that of face-centered cubic (fcc) Au (111) (0.235 nm) and fcc Cu (111) (0.209 nm), indicating that the coupling between Au NPs and Cu NWs via bipy does not affect NP/NW lattice structures.

The successful exchange of oleylamine with bipy on the NP and NW surfaces was characterized by infrared (IR) and ultra-violet-visible (UV-Vis) spectroscopy. IR spectra of the Au NPs and Cu NWs after the surfactant exchange show characteristic absorption peaks of bipy in 1400~1600 $cm^{-1}$ (C=N, C=C stretching) and 3000 $cm^{-1}$ (C-H stretching) (**Figure S3**).[7] The UV-Vis spectra show strong absorption of 4, 4'-bipyridine at 265 nm from free bipy, Cu-bipy and Au-bipy, not from the as-synthesized Cu NWs (**Figure S4**). The plasmonic absorption peaks of Au NPs at 526 nm and Cu NWs at 570 nm (**Figure 2a**) are unchanged upon the replacement of oleylamine by bipy. However, once Au NPs are landed on the Cu NW surface, the 570 nm Cu peak shifts slightly to 567 nm and Au NP plasmonic absorption becomes invisible due likely to the plasmonic coupling between Au and Cu,[8] indicating that Au and Cu are strongly coupled via bipy in the Au-bipy-Cu structure.

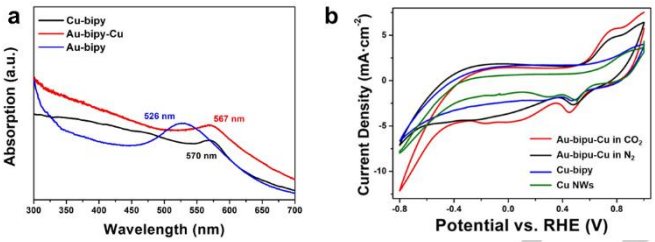


**Figure 2.** (a) UV-Vis spectra of Au-bipy, Cu-bipy, and Au-bipy-Cu. (b) CVs of Cu NWs, Cu-bipy, Au-bipy-Cu in $N_2$-saturated 0.1 M $KHCO_3$ and Au-bipy-Cu in $CO_2$-saturated 0.1 M $KHCO_3$.

Electrochemical properties of the carbon-supported Au-bipy-Cu were studied by cyclic voltammetry (CV) (see the Supporting Information for sample preparation). **Figure 2b** shows the CVs of Cu, Cu-bipy, and Au-bipy-Cu in $N_2$- and $CO_2$-saturated 0.1 M $KHCO_3$ (Au NPs have no redox peaks in the potential range we studied, **Figure S5**). Cu NWs have two typical reduction peaks at 0.5 V (Cu(II)/(Cu(I)) and 0.3 V (Cu(I)/Cu(0)).[9] When bipy binds to the Cu surface, both peaks shift cathodically to 0.47 V and 0.25 V respectively, and the Cu(I)/Cu(0) peak becomes weak and broad. When Cu-bipy is further modified with Au, as in Au-bipy-Cu, the Cu(I)/Cu(0) peak disappears. These indicate that the presence of bipy stabilizes Cu(II) and Cu(I) states more efficiently via the bipy bonding and shifts the Cu(I)-bipy reduction center from Cu(I) to bipy, which is further enhanced by Cu-bipy-Au interaction. These CV studies support what we have observed in the UV-Vis studies that bipy plays an important role in coupling Cu with Au in the Au-bipy-Cu structure. In the $CO_2$-saturated 0.1 M $KHCO_3$, the Cu(II)/Cu(I) peak shifts further cathodically and higher current is generated due to the $CO_2RR$ involved in the scanning process (**Figure 2b**).

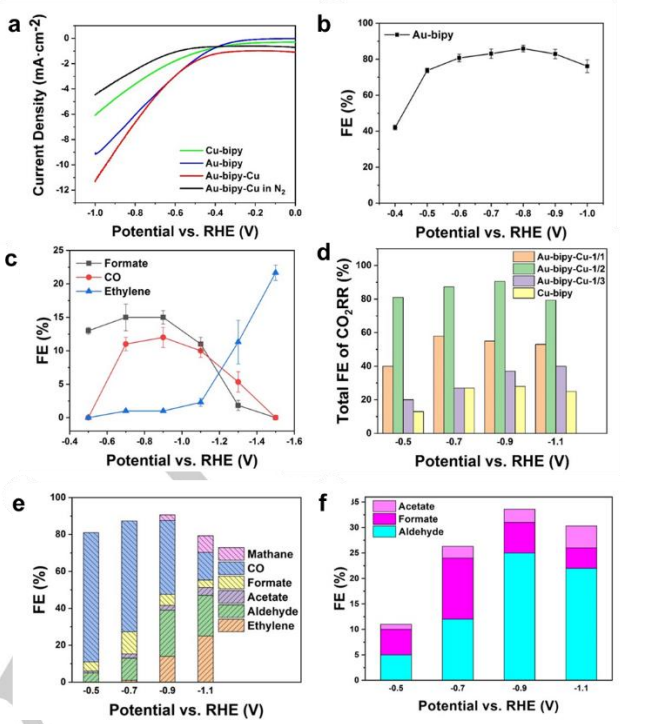


**Figure 3.** (a) LSV curves of Au-bipy-Cu catalysts in $N_2/CO_2$-saturated 0.1 M $KHCO_3$ solution and Au-bipy, Cu-bipy in $CO_2$-saturated 0.1 M $KHCO_3$ solution. (b) CO product FE of Au-bipy-catalyzed $CO_2RR$ at different potentials. (c) Product FEs of Cu-bipy-catalyzed $CO_2RR$ at different potentials. (d) Total FEs of Au-bipy-Cu-catalyzed $CO_2RR$ at different potentials. (e) Product FEs of Au-bipy-Cu-1/2-catalyzed $CO_2RR$ at different potentials. (f) FE of liquid products obtained from Au-bipy-Cu-1/2-catalyzed $CO_2RR$.

Linear scan voltammetry (LSV) measurements of Au-bipy, Cu-bipy, and Au-bipy-Cu catalysts in $N_2$- or $CO_2$-saturated 0.1 M $KHCO_3$ (**Figure 3a**) show these catalysts induce higher reduction currents at lower reduction potentials in the $CO_2$-saturated solution. The $CO_2RR$ catalyzed by Au-bipy produces CO with over 80% FE in −0.7 ~ −0.9 V (**Figure 3b**), similar to what was reported on Au NP catalysis for the $CO_2RR$ to CO.[2a] This indicates that the modification of Au NPs with bipy does not change the $CO_2RR$ selectivity of the 8 nm Au NPs. As a comparison, the Cu-bipy is less selective and its $CO_2RR$ catalysis yields CO (<12% FE) and formate (<15% FE), as well as $C_2H_4$ (<5%) in −0.6 ~ −1.1 V (**Figure 3c**). At a more negative reduction potential −1.2 V or beyond, the reaction selectivity is tuned more towards $C_2H_4$ with the FE increased steadily to 23% at −1.5 V, which is similar to what was observed in Cu NW-catalyzed $CO_2RR$.[5] The Au-bipy-Cu shows very different $CO_2RR$ activity and selectivity from either Au-bipy or Cu-bipy. First, the composite catalyst shows the Au/Cu mass ratio-dependent catalysis, and Au-bipy-Cu-1/2 is the most active catalyst for the $CO_2RR$ in all reduction potentials studied (**Figure 3d**). Second, the Au-bipy-Cu-1/2 catalyzes the $CO_2RR$ with an overall FE of C-products reaching 90.6% with the products containing CO, $HCOO^-$, $CH_4$, $C_2H_4$, $CH_3CHO$, and $CH_3COO^-$ (**Figure 3e**). To confirm all these carbons are from $CO_2$, not from bipy attached to the composite catalyst, we performed electrochemical reduction of $^{13}CO_2$ and the

representative $^{13}C$-products of $CH_3CHO$, $HCOO^-$, and $CH_3COO^-$ were characterized by negative electrospray ionization (ESI) high performance liquid chromatography-mass spectrometry (HPLC-MS) and $^1H$ nuclear magnetic resonance ($^1H$ NMR) spectroscopy (**Figure S7**). The peak of m-1/z = 45 can be assigned to $^{13}C$-labelled $CH_3CHO$, and that of m/z = 46 or 61 is from $^{13}C$-labelled $HCOO^-$ or $CH_3COO^-$ (**Figure S7a**). The presence of $^{13}C$ in $HCOO^-$ is further evidenced by presence of a proton doublet in the NMR spectrum of $HCOO^-$, which is the result of the H-$^{13}C$ coupling (**Figure S7b**). These support that the carbon source of the $CO_2RR$ products is from $CO_2$.[10] An interesting catalysis feature of the Au-bipy-Cu-1/2 is that at −0.5 V, the main product is CO (65% FE) due to the Au-catalyzed $CO_2RR$, and at more negative reduction potentials, Cu NWs are activated and CO FE is reduced, leading to the formation of multi-carbon products among which $C_2H_4$ and $CH_3CHO$ (as confirmed by $^1H$ NMR (**Figure S6**) are the main gas and liquid products respectively, which is different from the CO reduction reaction on the pure Cu NWs where only gaseous $C_2$-hydrocarbons ($C_2H_4$ + $C_2H_6$, 60% FE) were obtained.[5] The liquid products contain $HCOO^-$, $CH_3CHO$, and $CH_3COO^-$ (**Figure 3f**), and $CH_3CHO$ (25% FE) dominates the product distribution (75%), which is the highest aldehyde selectivity ever reported for the electrochemical reduction of $CO_2$ or CO.[3e, 11] During 6 h of continuous $CO_2RR$ at -0.9 V, we saw no current density drop from 13 $mA{\cdot}cm^{-2}$ (**Figure S8**) and the reaction FE stayed at 80%.

The Au-bipy-Cu catalyzed $CO_2RR$ shows Au/Cu mass ratio dependent catalysis. The $CO_2RR$ catalyzed Au-bipy-Cu-1/1 yielded only CO and $H_2$ (**Figure S9**). The presence of too many Au NPs shields the surface of Cu NWs, making the Au-bipy-Cu less effective as a composite catalyst for the $CO_2RR$. On the other hand, when the Au NPs are anchored only on a fraction of Cu NWs, as in Au-bipy-Cu-1/3, the $CO_2RR$ process is complicated and the products contain more $C_1$ (FE of < 30%) than $C_2$ products (FE < 15%) (**Figure S10**).

The tunable catalytic selectivity from Au-bipy, Cu-bipy to Au-bipy-Cu-1/2 on the $CO_2RR$ could be explained by the synergistic effect displayed by Au-bipy-Cu. Under the $CO_2RR$ condition, Au first catalyzes the $CO_2$ to CO at −0.5 V. As Cu is not activated at this potential, CO is the main gas product. At more negative potentials, Cu is activated and the Au-catalyzed $CO_2RR$ helps to enrich CO near the Cu NW surface. The synergistic effect of Au on Cu now turns the $CO_2RR$ to the CORR (Carbon Monoxide Reduction Reaction), which is known to facilitate CO-CO coupling. The conversion reaction is further enhanced by the presence of bipy Lewis base centers on the catalyst surface, which should help to stabilize the activated $CO_2$*[12] and enrich proton on the Cu catalyst surface, leading to highly selective conversion of $CO_2$ to C-products at a total FE of 90.6 % at −0.9 V.

In conclusion, we have demonstrated a new strategy of enhancing electrochemical $CO_2RR$ catalysis to C-products in 0.1 M $KHCO_3$ solution. The strategy involves assembly of Au NPs on Cu NWs via bipy, giving a new form of composite catalyst Au-bipy-Cu. The catalyst with Au/Cu mass ratio of 1/2 is the most efficient for converting $CO_2$ to C-products with a total FE reaching 90.6%. Among three different liquid products ($HCOO^-$, $CH_3CHO$, and $CH_3COO^-$) generated from the $CO_2RR$, $CH_3CHO$ has a FE fraction of 75%, the highest selectivity ever reported for the electrochemical $CO_2RR$ to aldehyde. The enhanced $CO_2RR$ catalysis of the Au-bipy-Cu originates from the synergistic effects among Au (for $CO_2$ to CO), Cu (for CO coupling) and bipy (for the $CO_2$* stabilization and protonation). The assembly strategy demonstrated here can be easily extended to prepare many other composite catalysts, making it possible to tune and optimize their catalysis for $CO_2RR$ to specific hydrocarbons or oxygenated hydrocarbons.

## Acknowledgements

The work at Brown University was supported by the American Chemical Society Petroleum Research Fund (57114-ND5) and in part by the Center for the Capture and Conversion of $CO_2$, a Center for Chemical Innovation funded by the National Science Foundation, CHE-1240020. We thank the International Cooperation Foundation from Ministry of Science and Technology of China (2016YFE0130100), National Natural Science Foundation of China (21834004) and the program B for Outstanding PhD candidate of Nanjing University (Nos. 201801B024 and 201801B025) for support. The authors would like to thank Chuan Chai at Nanjing University of Chinese Medicine for the help on HPLC-MS analysis.

**Keywords:** Electrocatalysis • $CO_2$ reduction • Nanoparticles • keyword 4 • keyword 5

[1] a) Z. W. Seh, J. Kibsgaard, C. F. Dickens, I. Chorkendorff, J. K. Nørskov, T. F. Jaramillo, *Science* **2017**, *355*, eaad4998; b) Y. Jiao, Y. Zheng, K. Davey, S.-Z. Qiao, *Nat. Energy* **2016**, *1*, 16130; c) Q. J. Xiang, B. Cheng, J. G. Yu, *Angew. Chem. Int. Edit.* **2015**, *54*, 11350-11366; d) D. Voiry, H. S. Shin, K. P. Loh, M. Chhowalla, *Nat. Rev. Chem.* **2018**, *2*, 0105.

[2] a) W. Zhu, R. Michalsky, Ö. Metin, H. Lv, S. Guo, C. J. Wright, X. Sun, A. A. Peterson, S. Sun, *J. Am. Chem. Soc.* **2013**, *135*, 16833-16836; b) W. Zhu, L. Zhang, P. Yang, C. Hu, Z. Luo, X. Chang, Z.-J. Zhao, J. Gong, *Angew. Chem. Int. Edit.* **2018**, *57*, 11544-11548; c) R. Francke, B. Schille, M. Roemelt, *Chem. Rev.* **2018**, *118*, 4631-4701; d) M. Liu, Y. J. Pang, B. Zhang, P. De Luna, O. Voznyy, J. X. Xu, X. L. Zheng, C. T. Dinh, F. J. Fan, C. H. Cao, F. P. G. de Arquer, T. S. Safaei, A. Mepham, A. Klinkova, E. Kumacheva, T. Filleter, D. Sinton, S. O. Kelley, E. H. Sargent, *Nature* **2016**, *537*, 382-386; e) J. Medinaramos, R. C. Pupillo, T. P. Keane, J. L. Dimeglio, J. Rosenthal, *J. Am. Chem. Soc.* **2015**, *137*, 5021-5027; f) T. Hatsukade, K. P. Kuhl, E. R. Cave, D. N. Abram, T. F. Jaramillo, *Phys. Chem. Chem. Phys.* **2014**, *16*, 13814-13819.

[3] a) Y. Hori, K. Morden Aspects of Electrochemistry, *No. 42* (Eds: C.G. Vayenas, R.E. White, M. E. Gamboa-Aldeco), Springer, New York, **2008**, pp. 88-189; b) H. Xie, T. Y. Wang, J. S. Liang, Q. Li, S. H. Sun, *Nano Today* **2018**, *21*, 41-54; c) H. Jung, S. Y. Lee, C. W. Lee, M. K. Cho, D. H. Won, C. Kim, H.-S. Oh, B. K. Min, Y. J. Hwang, *J. Am. Chem. Soc.* **2019**, *141*, 4624-4633; d) Z. Q. Liang, T. T. Zhuang, A. Seifitokaldani, J. Li, C. W. Huang, C. S. Tan, Y. Li, P. De Luna, C. T. Dinh, Y. F. Hu, Q. F. Xiao, P. L. Hsieh, Y. H. Wang, F. W. Li, R. Quintero-Bermudez, Y. S. Zhou, P. N. Chen, Y. J. Pang, S. C. Lo, L. J. Chen, H. R. Tan, Z. Xu, S. L. Zhao, D. Sinton, E. H. Sargent, *Nat. Commun.* **2018**, *9*, 3828; e) A. Loiudice, P. Lobaccaro, E. A. Kamali, T. Thao, B. H. Huang, J. W. Ager,

10.1002/anie.201905318


R. Buonsanti, *Angew. Chem. Int. Edit.* **2016**, *55*, 5789-5792; f) A. Vasileff, C. C. Xu, Y. Jiao, Y. Zheng, S. Z. Qiao, *Chem* **2018**, *4*, 1809-1831.

[4] a) M. Jouny, W. Luc, F. Jiao, *Nat. Catal.* **2018**, *1*, 748-755; b) K. P. Kuhl, E. R. Cave, D. N. Abram, T. F. Jaramillo, *Energy Environ. Sci.* **2012**, *5*, 7050-7059; c) H. Xiao, T. Cheng, W. A. Goddard, R. Sundararaman, *J. Am. Chem. Soc.* **2016**, *138*, 483-486; d) C. W. Li, J. Ciston, M. W. Kanan, *Nature* **2014**, *508*, 504-507.

[5] H. Zhang, Y. Zhang, Y. Li, S. Ahn, G. T. R. Palmore, J. Fu, A. A. Peterson, S. Sun, *Nanoscale,* **2019**, *11*,12075-12079.

[6] E. Ye, S. Y. Zhang, S. Liu, M. Y. Han, *Chem.-Eur. J.* **2011**, *17*, 3074-3077.

[7] L. OuldMoussa, O. Poizat, M. CastellaVentura, G. Buntinx, E. Kassab, *J. Phys. Chem.* **1996**, *100*, 2072-2082.

[8] a) D. Zhao, X. Xiong, C. L. Qu, N. Zhang, *J. Phys. Chem. C* **2014**, *118*, 19007-19016; b) C. L. Bracey, P. R. Ellis, G. J. Hutchings, *Chem. Soc. Rev.* **2009**, *38*, 2231-2243.

[9] a) Y. Wan, Y. D. Zhang, X. L. Wang, Q. Wang, *Electrochem. Commun.* **2013**, *36*, 99-102; b) Q. Li, J. J. Fu, W. L. Zhu, Z. Z. Chen, B. Shen, L. H. Wu, Z. Xi, T. Y. Wang, G. Lu, J. J. Zhu, S. H. Sun, *J. Am. Chem. Soc.* **2017**, *139*, 4290-4293.

[10] Y. Tamaki, T. Morimoto, K. Koike, O. Ishitani, *Proc. Natl. Acad. Sci. U. S. A.* **2012**, *109*, 15673–15678.

[11] E. Bertheussen, T. V. Hogg, Y. Abghoui, A. K. Engstfeld, I. Chorkendorff, I. E. L. Stephens, *ACS Energy Lett.* **2018**, *3*, 634-640.

[12] B. A. Rosen, A. Salehi-Khojin, M. R. Thorson, W. Zhu, D. T. Whipple, P. J. A. Kenis, R. I. Masel, *Science* **2011**, *334*, 643-644.

10.1002/anie.201905318

WILEY-VCH



COMMUNICATION

The electrochemical reduction of $CO_2$ to hydrocarbons is enhanced by assembling Au nanoparticles and Cu nanowires via bipyridine, which provide the synergistic effects among Au (for $CO_2$ to CO), Cu (for CO coupling) and bipy (for the $CO_2$* stabilization and protonation).

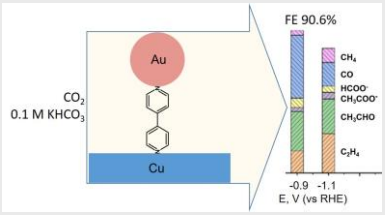


*Jiaju Fu, Wenlei Zhu, Ying Chen, Zhouyang Yin, Yuyang Li, Juan Liu, Hongyi Zhang, Jun-Jie Zhu* and Shouheng Sun**

***Page No. – Page No.***

**Bipyridine-assisted assembly of Au nanoparticles on Cu nanowires to enhance electrochemical reduction of $CO_2$**